Design of a molecular clock with RNA–mediated regulation

Franco Blanchini[1], Christian Cuba Samaniego[2], Elisa Franco[2] and Giulia Giordano[1]

Abstract— We design a new negative feedback molecular oscillator and study its properties analytically and numerically. This oscillator is composed of two synthetic genes interconnected through their RNA outputs. Regulation of the genes activity is achieved by controlling the activity of the enzymes rather than the activity of the promoters. We show that a simple model of this system has the potential to oscillate for appropriate choices of the parameters. Our design can be built experimentally using RNA aptamers.

I. INTRODUCTION

Nucleic acids are versatile molecular polymers, whose thermodynamic and kinetic interactions can be programmed exploiting Watson-Crick base pairing rules. By programming the sequence content of ensembles of single stranded NA species, we can specify their interactions and the dynamics of such interactions. Using this simple principle, a variety of dynamic and logic circuits have been recently demonstrated experimentally [1], [2], [3], [4]. Potentially, we can create arbitrary biomolecular circuit architectures having desired dynamics [5].

In this and a companion paper [6], we propose to create a molecular oscillator and a toggle switch, two canonical biological dynamic networks, using RNA species designed to change the activity of the enzymes producing them. These RNA sequences capable of binding a target and changing its properties are known as aptamers [7]; aptamers binding to a specific target can be obtained systematically by randomized evolution techniques. In particular, it is possible to use aptamers to inactivate RNA polymerases, enzymes responsible for RNA transcription [8], [9]. Based on the availability of these aptamers, we propose to design a negative feedback oscillator where regulation is achieved by modulating enzyme activity. Unlike recently proposed *in vitro* oscillators [2], [4], our design has the potential to work *in vitro* because it relies only on reaction pathways naturally present in the cellular environment.

The structure of previously proposed *in vitro* oscillators is also based on the creation of a negative feedback loop, destabilized by the presence of reactions causing a delay [10], [2] or by a positive feeedback loop [4]. Our oscillator is based on transcription reactions as the oscillator studied in [10], [2], however we consider a very different type of regulation: instead of modulating the activity of

[1]F. Blanchini and G. Giordano are with the Department of Mathematics and Computer Science, Università degli Studi di Udine, Udine, Italy. blanchini@uniud.it, giulia.giordano@uniud.it

[2]C. Cuba Samaniego and E. Franco are with the Department of Mechanical Engineering, University of California Riverside, California 92502, USA. ccuba002@ucr.edu, efranco@engr.ucr.edu

the promoters, we modulate the activity of the enzymes performing transcription.

We study this proposed oscillator design analytically, employing classical control theoretic methods [11], [12], [13], [14], and numerically. We note that the model proposed here is not mechanistic nor exhaustive, but rather a simplified set of differential equations that capture the main reactions at the core of our design. Our analysis shows that this system is a candidate oscillator. A thorough randomized search for parameters yielding an oscillatory behavior returns reaction rates that fall within a realistic range for experimental implementation. We focus on the role of RNA transcription rates, which are difficult to control, and enzyme decay/recovery rates, which will be engineered in the laboratory.

II. CIRCUIT DESCRIPTION AND MODELING

Biochemical oscillators are designed with a simple general principle: a series of reactions must generate a negative feedback loop with suitable delay or positive feedback loop to destabilize the system [15]. We focus on *in vitro* transcription reactions, and we use RNA inputs to regulate the ability of synthetic genes to generate RNA outputs. Regulation of transcription is achieved by modulating the activity of RNA polymerases (RNAP), rather than the activity of promoters. Using specific RNA aptamers (short, noncoding RNA sequences that bind a desired target [16], [17]) we can inhibit the activity of two well characterized and commercially available bacteriophage RNAP species [8], [9].
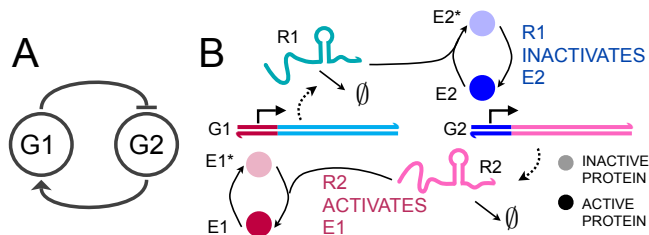
Fig. 1. A: General cheme of a two node transcriptional oscillator; G_1 and G_2 are associated to genes. B: Proposed experimental implementation of an RNA-based clock, where the transcription enzymes are directly inhibited or activated by RNA aptamers.

As shown in Fig. 1, our scheme is based on two synthetic genes producing RNA outputs R_1 and R_2. The RNA outputs are transcribed by two different enzymes E_1 and E_2; for example, one could use bacteriophage SP6 and T7 RNAPs, and the corresponding promoter sequences (purple and blue domains on the genes in Fig. 1). We assume that enzymes can either be in an active or inactive state, and their mass

is conserved: $[E_i^{tot}] = [E_i] + [E_i^*]$, $i = 1, 2$. Enzyme E_2 is inhibited by RNA species R_1 (through a direct aptamer binding pathway), and it reverts to its active state at a given rate which could be driven by a strand displacement reaction [18] (*i.e.* another RNA or DNA specie binds to R_1 and releases the enzyme). Conversely, we assume that enzyme E_1 is activated by R_2, and it decays at a given rate: direct activation through an aptamer is not currently possible, but R_2 could act as a species displacing an inhibiting aptamer. Since mechanisms to implement the enzyme decay/recovery reactions are currently being researched, we will focus on their role in achieving oscillations. We will contrast the role of these reaction rates with the RNA transcription rates, which depend on the chosen protein and are difficult to engineer.

The overall list of reactions is:

$$E_i + g_i \xrightarrow{k_i} E_i + R_i + g_i \quad \text{RNA production}, i = 1, 2$$
$$R_i \xrightarrow{\delta_i} 0 \quad \text{RNA degradation}, i = 1, 2$$
$$E_1^* + R_2 \xrightarrow{\gamma_1} E_1 \quad \text{Activation}$$
$$E_1 \xrightarrow{\beta_1} E_1^* \quad \text{Decay}$$
$$E_2 + R_1 \xrightarrow{\gamma_2} E_2^* \quad \text{Inhibition}$$
$$E_2^* \xrightarrow{\beta_2} E_2 \quad \text{Recovery}$$
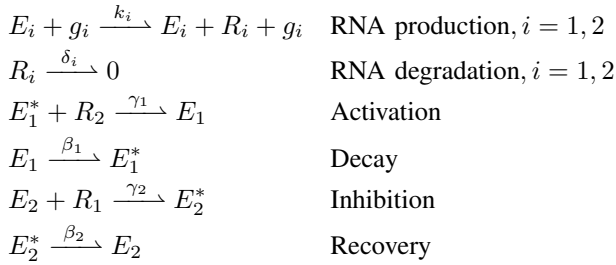
where E_i are active enzymes, E_i^* are inactive enzymes, R_i are RNA species, g_i are genes (constant). In this paper, we neglect the contribution of additional species required to implement the decay and recovery reactions.

Using mass action kinetics, we can derive the ordinary differential equations (ODEs) describing the dynamics of the system:

$$[\dot{R_1}] = k_1[E_1][g_1] - \delta_1[R_1] - \gamma_2([E_2])[R_1]$$
$$[\dot{E_1}] = -\beta_1[E_1] + \gamma_1([E_1^{tot}] - [E_1])[R_2]$$
$$[\dot{R_2}] = k_2[E_2][g_2] - \delta_2[R_2] - \gamma_1([E_1^{tot}] - [E_1])[R_2]$$
$$[\dot{E_2}] = \beta_2([E_2^{tot}] - [E_2]) - \gamma_2[E_2][R_1]$$

We now switch to a more compact notation $x_1 := [R_1]$, $x_2 := [E_1]$, $x_3 := R_2$ and $x_4 := E_2$. Because the concentration of genes is constant, we also define lumped parameters $\kappa_i = k_i[g_i]$, and we rewrite the equations above as:

$$\begin{cases} \dot{x_1} = \kappa_1 x_2 - \delta_1 x_1 - \gamma_2 x_4 x_1 \\ \dot{x_2} = -\beta_1 x_2 + \gamma_1(x_2^{tot} - x_2)x_3 \\ \dot{x_3} = \kappa_2 x_4 - \delta_2 x_3 - \gamma_1(x_2^{tot} - x_2)x_3 \\ \dot{x_4} = \beta_2(x_4^{tot} - x_4) - \gamma_2 x_4 x_1 \end{cases} \quad (1)$$

In the next sections, we analytically show that model (1) can exhibit oscillations, and we numerically explore its oscillatory domain. An interesting result of our numerical simulations is that κ_1 (production rate of R_1) and β_2 (recovery rate of E_2) should be proportional on a logarithmic scale to yield an oscillatory behavior. This result and other trends in parameter space, identified in Fig. 6, will be useful for the experimental implementation of the oscillator.

III. STABILITY ANALYSIS

We begin our analysis by stating the following boundedness result.

Proposition 1: The solutions of system (1) are bounded for any nonnegative initial condition such that $x_2(0) \leq x_2^{tot}$ and $x_4(0) \leq x_4^{tot}$.

Proof: The bounds $0 \leq x_2(t) \leq x_2^{tot}$ and $0 \leq x_4(t) \leq x_4^{tot}$ are immediately derived from the second and the fourth equations in (1). Now consider the quantities $x_1^+ = \frac{\kappa_1}{\delta_1}x_2^{tot}$ and $x_3^+ = \frac{\kappa_2}{\delta_2}x_4^{tot}$. As long as the conditions $0 \leq x_1(t) \leq x_1^+$ and $0 \leq x_3(t) \leq x_3^+$ are satisfied for $t = 0$, they will be fulfilled for each time $t > 0$. Furthermore, these conditions are asymptotically satisfied for any initial state. Indeed, for x_1 we have: $\dot{x_1} \leq \kappa_1 x_2 - \delta_1 x_1 \leq \kappa_1 x_2^{tot} - \delta_1 x_1$. From this differential inequality, we see that the solution $x_1(t)$ is upper bounded by the solution of $\dot{x_1} = \kappa_1 x_2^{tot} - \delta_1 x_1$, hence $x_1(t) \leq x_1^+ + [x_1(0) - x_1^+]e^{-\delta_1 t}$. Similarly, we can show that $x_3(t) \leq x_3^+ + [x_3(0) - x_3^+]e^{-\delta_2 t}$. ∎

Boundedness implies the existence of an equilibrium point inside the nonnegative box delimited by the quantities x_1^+, x_2^{tot}, x_3^+, x_4^{tot} ([19], see also [20], [21]). We perform our stability analysis by finding equilibrium conditions for model (1). Setting $\dot{x_2} = 0$ we find

$$x_3 = \frac{\beta_1 x_2}{\gamma_1(x_2^{tot} - x_2)},$$

which can be substituted into equation $\dot{x_3} = 0$, yielding an expression of x_4 as a function of x_2:

$$x_4 = f(x_2) = \frac{1}{\kappa_2}\left[\frac{\delta_2\beta_1 x_2}{\gamma_1(x_2^{tot} - x_2)} + \beta_1 x_2\right].$$

Similarly, from $\dot{x_4} = 0$ we get

$$x_1 = \frac{\beta_2(x_4^{tot} - x_4)}{\gamma_2 x_4},$$

which, substituted in equation $\dot{x_1} = 0$, yields an expression of x_2 as a function of x_4:

$$x_2 = g(x_4) = \frac{1}{\kappa_1}\left[\frac{\delta_1\beta_2(x_4^{tot} - x_4)}{\gamma_2 x_4} + \beta_2(x_4^{tot} - x_4)\right].$$

The equilibrium conditions in the variables x_2 and x_4 are represented in Fig. 2. Parameters used for this plot are in Table I, and are realistic for *in vitro* synthetic networks [22]. Due to the monotonic trend of the equilibrium conditions (f is increasing and g is decreasing), the following proposition is immediate.

Proposition 2: System (1) admits a single equilibrium.

We now proceed with a structural analysis, which is useful to find local stability results. The Jacobian matrix

$$J = \begin{bmatrix} -\gamma_2\bar{x}_4 - \delta_1 & \kappa_1 & 0 & -\gamma_2\bar{x}_1 \\ 0 & -\beta_1 - \gamma_1\bar{x}_3 & \gamma_1(x_2^{tot} - \bar{x}_2) & 0 \\ 0 & \gamma_1\bar{x}_3 & -\gamma_1(x_2^{tot} - \bar{x}_2) - \delta_2 & \kappa_2 \\ -\gamma_2\bar{x}_4 & 0 & 0 & -\beta_2 - \gamma_2\bar{x}_1 \end{bmatrix}$$

is sign definite and, through a state transformation

$$T = \begin{bmatrix} 0 & 0 & 0 & -1 \\ 0 & 1 & 0 & 0 \\ 1 & 0 & 0 & 0 \\ 0 & 0 & 1 & 0 \end{bmatrix},$$
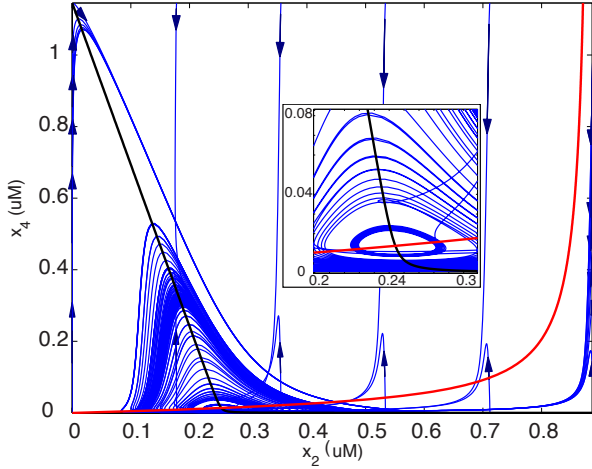
Fig. 2. Phase plane and equilibrium conditions for a series of trajectories of model (1) using parameters in Table I (Table II shows the same parameters expressed in different units) . The red line corresponds to $x_4 = f(x_2)$ and the black line to $x_2 = g(x_4)$. This plot corresponds to the black diamond in all panels of Fig. 7.

it is similar to a matrix $\tilde{J} = T^{-1}JT$:

$$\tilde{J} = \begin{bmatrix} -\gamma_1(x_2^{tot} - \bar{x}_2) - \delta_2 & \gamma_1\bar{x}_3 & \kappa_2 & 0 \\ \gamma_1(x_2^{tot} - \bar{x}_2) & -\beta_1 - \gamma_1\bar{x}_3 & 0 & 0 \\ 0 & 0 & -\beta_2 - \gamma_2\bar{x}_1 & \gamma_2\bar{x}_4 \\ 0 & -\kappa_1 & \gamma_2\bar{x}_1 & -\gamma_2\bar{x}_4 - \delta_1 \end{bmatrix}.$$

The new state vector corresponding to the transformed $\tilde{J}$ is:

$$\begin{aligned}\zeta &= \begin{bmatrix} \zeta_1 & \zeta_2 & \zeta_3 & \zeta_4 \end{bmatrix}^\top \\ &= \begin{bmatrix} (x_3 - \bar{x}_3) & (x_2 - \bar{x}_2) & (x_4 - \bar{x}_4) & -(x_1 - \bar{x}_1) \end{bmatrix}^\top.\end{aligned}$$

As it is emphasized by this transformation, the overall system is the negative feedback interconnection of two subsystems (respectively governed by the variables x_3–x_2 and x_4–x_1) which are input–output monotone with respect to the positive orthant and which are both stable. This means that instability can only occur due to a complex pair of unstable poles. In other words, the system admits only oscillatory transitions to instability [23]. This can be seen either by calculating the coefficients of the characteristic polynomial, which are all positive, or by means of the following considerations.

To recap, we have seen that:
- every solution of the overall system is bounded;
- the overall system is the positive feedback interconnection of two subsystems which are input–output monotone and anti–monotone respectively;
- the input–output characteristics of the two subsystems, $x_2 = f^{-1}(x_4)$ and $x_4 = g^{-1}(x_2)$, are monotonically increasing and decreasing, respectively.

Therefore, according to Theorem 3 in [11], the overall system has a globally attractive equilibrium if the scalar discrete–time system

$$x_4^{k+1} = (g^{-1} \circ f^{-1})(x_4^k) \tag{2}$$

has a globally attractive fixed point.

This criterion offers as a sufficient condition for local stability that the iterated values of the discrete system (2)

locally converge. Hence, a necessary condition to have sustained oscillations is that the iterated values of (2) *diverge*. This is equivalent to local convergence of the discrete–time system

$$x_4^{k-1} = (f \circ g)(x_4^k). \tag{3}$$

Local convergence of iterations is assured if the derivative of the overall function is smaller than 1 in absolute value. Thus, our necessary condition for oscillations can be expressed as

$$-\frac{df(x_2)}{x_2}\frac{dg(x_4)}{x_4} < 1$$

or, equivalently, as

$$-\frac{df^{-1}(x_4)}{x_4}\frac{dg^{-1}(x_2)}{x_2} > 1.$$

The minus sign is due to the fact that $\frac{dg(x_4)}{x_4} < 0$ and $\frac{dg^{-1}(x_2)}{x_2} < 0$.

We have seen that the iteration method provides a necessary condition for the onset of oscillations. This method will be numerically implemented in Section IV-A to analyze our model. A criterion based on linearizion, which we will discuss in the following subsection, may seem preferable. However, two basic facts have to be considered.

- The iteration method provides an insight about the oscillatory condition. In essential, for the oscillations to occur, it is necessary that at the intersection point the derivatives of both the curves $x_4 = f(x_2)$ and $x_2 = g(x_4)$, i.e. $df(x_2)/dx_2$ and $dg(x_4)/dx_4$, are large in magnitude.
- Perhaps more importantly, the fourth–order model we consider is simple and suitable for analysis, but too simplified to provide a faithful representation of the phenomenon. In particular, the chain of reactions involved in the true process may include delays, which this model neglects. The presence of delays does not affect the iteration method, as long as we can assume that the overall system is the feedback interconnection of two subsystems which are monotone and anti–monotone.

A. Local linearized analysis

We now consider the transformed Jacobian matrix $\tilde{J}$ and proceed with a local linear analysis. We linearize the first subsystem, obtaining matrices

$$A_1 = \begin{bmatrix} -\gamma_1(x_2^{tot} - \bar{x}_2) - \delta_2 & \gamma_1\bar{x}_3 \\ \gamma_1(x_2^{tot} - \bar{x}_2) & -\beta_1 - \gamma_1\bar{x}_3 \end{bmatrix},$$

$$B_1 = \begin{bmatrix} \kappa_2 \\ 0 \end{bmatrix}, \quad C_1 = \begin{bmatrix} 0 & 1 \end{bmatrix},$$

where the state vector is $\begin{bmatrix} \zeta_1 & \zeta_2 \end{bmatrix}^\top$, the input is ζ_3 and the output is ζ_2. The second linearized subsystem is represented by matrices

$$A_2 = \begin{bmatrix} -\beta_2 - \gamma_2\bar{x}_1 & \gamma_2\bar{x}_4 \\ \gamma_2\bar{x}_1 & -\gamma_2\bar{x}_4 - \delta_1 \end{bmatrix},$$

$$B_1 = \begin{bmatrix} 0 \\ -\kappa_1 \end{bmatrix}, \quad C_2 = \begin{bmatrix} 1 & 0 \end{bmatrix},$$

where the state is $\begin{bmatrix} \zeta_3 & \zeta_4 \end{bmatrix}^\top$, the input is ζ_2 and the output is ζ_3.

We can notice that, since both of the monotone linearized subsystems are associated with a strongly diagonally dominant Metzler matrix, they both are locally stable.
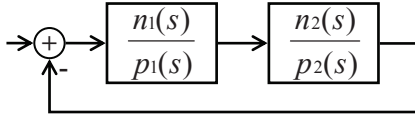
Fig. 3. Block diagram of the overall system, represented as the negative feedback interconnection of two monotone subsystems.

The overall linearized system is the negative feedback interconnection (Fig. 3) of the two linearized subsystems above, which are associated with the transfer functions

$$F_1(s) = \frac{n_1(s)}{p_1(s)}, \qquad F_2(s) = \frac{n_2(s)}{p_2(s)},$$

where

$$n_1(s) = \kappa_2 \gamma_1 (x_2^{tot} - \bar{x}_2),$$
$$p_1(s) = s^2 + [\beta_1 + \delta_2 + \gamma_1 \bar{x}_3 + \gamma_1 (x_2^{tot} - \bar{x}_2)]s + $$
$$+ [\beta_1 \delta_2 + \beta_1 \gamma_1 (x_2^{tot} - \bar{x}_2) + \gamma_1 \delta_2 \bar{x}_3],$$
$$n_2(s) = \kappa_1 \gamma_2 \bar{x}_4,$$
$$p_2(s) = s^2 + (\beta_2 + \delta_1 + \gamma_2 \bar{x}_1 + \gamma_2 \bar{x}_4)s + $$
$$+ (\beta_2 \delta_1 + \beta_2 \gamma_2 \bar{x}_4 + \gamma_2 \delta_1 \bar{x}_1).$$

Of course, the characteristic polynomial of the overall system is equal to the denominator of the closed loop transfer function:

$$p(s) = p_1(s)p_2(s) + n_1(s)n_2(s) = $$
$$= p_1(s)p_2(s) + \kappa_1 \kappa_2 \gamma_1 \gamma_2 (x_2^{tot} - \bar{x}_2)\bar{x}_4.$$

Since all the coefficients of $p(s)$ are positive, the system does not admit real positive eigenvalues; therefore, if it becomes unstable, instability must be oscillatory. By computing the Routh–Hurwitz table, it is possible to verify that, for some choice of the parameters, instability can only occur due to two unstable eigenvalues, which must correspond to a complex pair of eigenvalues.

IV. NUMERICAL ANALYSIS

A. Iteration method

We have implemented the iteration method discussed in Section III in order to analyze system (1) and show that, for a suitable range of parameters, the necessary condition for sustained oscillations is actually verified.

Fig. 4 shows the equilibrium conditions $x_4 = f(x_2)$ and $x_2 = g(x_4)$, for the nominal parameter values shown in Table II, and the convergence of the counterclockwise (backward) iteration $x_4^{k-1} = (f \circ g)(x_4^k)$ to the equilibrium point. It is possible to verify that, for these parameter values, the system Jacobian has a complex pair of unstable eigenvalues, thus oscillations actually arise.

Fig. 5 shows the result of an iteration–convergence test and of the eigenvalues computation for a wider interval
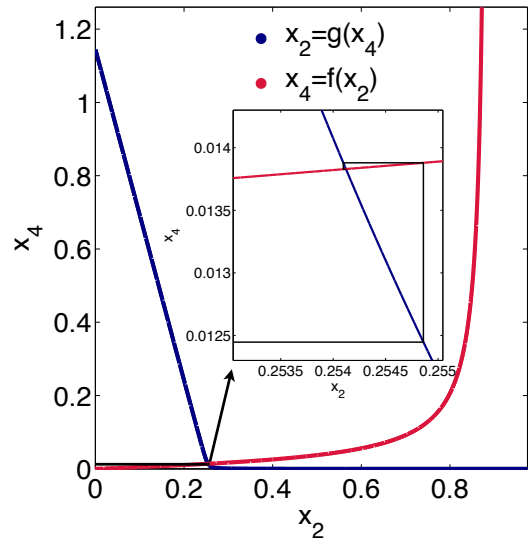
Fig. 4. Convergence of the counterclockwise (backward) iteration $x_4^{k-1} = (f \circ g)(x_4^k)$ to the equilibrium point for the system with the nominal parameters shown in Table II; convergence is a necessary condition for oscillations. The inset shows a magnification of the iteration near the equilibrium.

of parameters: while the other parameters are kept as in Table II, β_1 and κ_1 are logarithmically varied from 0.1 to 10 times their nominal value. In Fig. 5 (a), the blue area represents parameter choices for which the iteration procedure converges (which is a necessary condition for oscillations), while in Fig. 5 (b) the blue area represents parameter choices for which the system Jacobian admits a complex pair of unstable eigenvalues (which means that the system does in fact oscillate). As expected, the oscillatory domain is completely included in the convergence domain.

B. Randomized parameter search

We set up a numerical simulation to find parameter sets that yield an oscillatory behavior in model (1). We generated random parameters values starting from the nominal parameter set listed on Table II. We generated several hundreds additional random parameter sets, in the range from 10^{-3} to 10^3 times their nominal values, except for x_2^{tot} and x_4^{tot}, which are in the range from 10^{-1} to 10^1 times their nominal values listed on Table II. Then, the differential equations are solved using the deterministic integrator RADAU, included in the software PyDSTool [24]. A paramter set is considered acceptable if the period of the resulting oscillations beween $0.5h$ and $10h$, and the amplitude is larger than 1 nM. When integrating our ODEs, we assumed initial conditions $x_1(0) = 0$, $x_3(0) = 0$, $x_2(0) = x_2^{tot}$ and $x_4(0) = x_4^{tot}$.

Period and amplitude were computed by identifying minima and maxima of oscillations, as shown in the inset of Fig. 6 (c). Maxima and minima are identified as follows. For each three consecutive points of a trajectory, we define $d1$ and $d2$ as shown in Fig. 6 (b): $d1 = p_n - p_{n-1}$ and $d2 = p_n - p_{n+1}$. If the product $d1 \cdot d2$ is positive and $d1$ is positive, then p_n is classified as a local maximum; if $d1$ is negative, then p_n is classified as a local minimum. Period

(a) Parameter choices which guarantee convergence

(b) Parameter choices which guarantee sustained oscillations
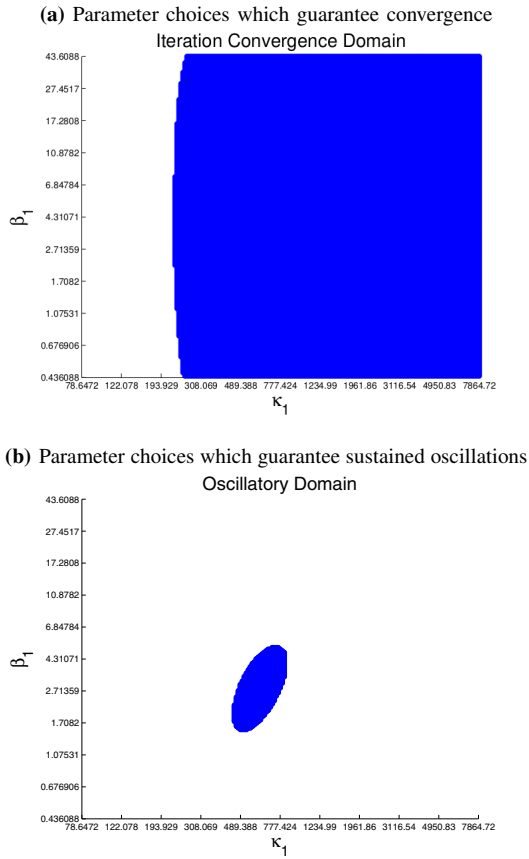
Fig. 5. Simulations which show (a) the iteration convergence domain and (b) the oscillatory domain, consistent with Fig. 7. β_1 and κ_1 vary from 0.1 to 10 times their nominal value, while the other parameter values are those in Table II. The blue region in panel (b) is entirely included in the blue region in panel (a), as it must be, since convergence is a necessary condition for oscillations.

Fig. 6. (a): Dark points mark parameter combinations that yield oscillations in the system. Parameters variations are on a logarithmic scale relative to the parameters listed in Table II. (b) and (c): sketch of our criteria to identify maxima and minima, and to mesure period and amplitude.

and amplitude are computed from the identified maxima and minima, as sketched in Fig. 6 (c). Period and amplitude are averaged over all the different measured peaks and wells and compared to the aforementioned thresholds.

In Fig. 6 (a) we show the correlations among pairs of parameters that yield oscillations. Some of these correlations show clear patterns. For example κ_1 (production rate of R_1) and β_2 (recovery rate of E_2) should be proportional on a logarithmic scale. For the chosen parameter set, this relationship is quite critical. Also, β_1 (decay rate of E_1), δ_2 (degradation rate of R_2) and γ_2 (inhibition rate of E_2) exhibit a minimum threshold level. We recall that β_1 and β_2 are the enzymes recovery and decay rates, whose exact mechanisms of implementation are still under investigation, and thus are particularly relevant in our analysis.

C. Classification of dynamic behaviors in a region of the parameter space

Given a certain parameter set, we classify parameter that yield a 'spiral source', 'spiral sink' and 'sink node' behavior, checking the eigenvalues of the system linearized around its only equilibrium. Starting from the nominal parameters listed in Table II, each parameter is varied from 0.1 to 10 times its

nominal value. Then, the equilibrium points are computed to find the eigenvalues from its Jacobian.

We summarize our results in Fig. 7, which shows the influence of the parameters on the stability properties of the unique equilibrium of the system. The classification is color coded as follows (legend is also shown in Fig. 7): points at which we find real and negative eigenvalues are shown in blue color; points where at least one eigenvalue is complex with negative real part are shown in orange color; points where at least one eigenvalue is complex with positive real part are shown in grey color.

This plot will be a useful guide for tuning experimental parameters without losing the oscillatory behavior. The plot also identifies critical parameter combinations which should not be changed beyond a narrow range. In particular, we observe that κ_1 and β_2 must be proportional as in Fig. 6. We note that this plot summarizes local stability properties, and thus provides less general information than Fig. 6 which is obtained simulating the full nonlinear system. We conclude observing that the relationship between parameters κ_1 and β_1 found in Fig. 6 is consistent with the oscillatory domain found at Fig. 5 using the iteration method described in Section III. The κ_1/β_1 region in which the linearized system admits oscillations is quite narrow given the chosen combination of paramters.

V. CONCLUSION

We have proposed the design of a molecular oscillator where a negative feedback loop is created by modulating enzymatic activity through RNA aptamers. Our analysis and
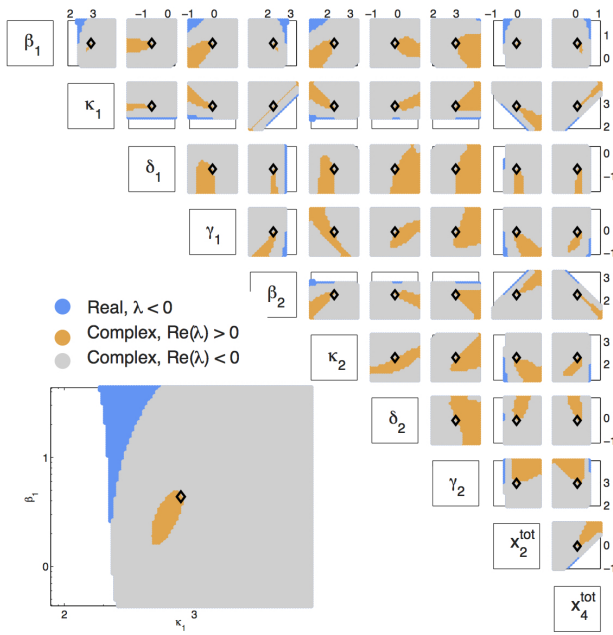
Fig. 7. Stability of the equilibrium, parameters are varied on a logarithmic scale; the black diamond represent the parameters shown in Table (II). The central panel shows the results for varying β_1 and κ_1, and is consistent with the results of Fig. 5.

TABLE I
SIMULATION PARAMETERS, IN UNITS OF M AND s

β_1 1/s	κ_1 1/s	δ_1 1/s	γ_1 1/Mol.s	x_2^{tot} μM
1.211e-3	0.219	5.53e-5	2.297e2	0.886
β_2 1/s	κ_2 1/s	δ_2 1/s	γ_2 1/Mol.s	x_4^{tot} μM
4.832e-2	5.422e-2	2.085e-4	2.599e5	1.145

TABLE II
SIMULATION PARAMETERS SHOWN IN TABLE I, CONVERTED TO UNITS OF μM AND h

β_1 1/h	κ_1 1/h	δ_1 1/h	γ_1 1/μM.h	x_2^{tot} μM
4.3609	786.4720	0.1991	0.8270	0.886
β_2 1/h	κ_2 1/h	δ_2 1/h	γ_2 1/μM.h	x_4^{tot} μM
173.9377	195.1742	0.7504	935.6293	1.145

numerical simulations show that the proposed architecture exhibits oscillations for appropriate parameter choices, albeit for the chosen region in parameter space the required relationship between certain parameters are tight. We are actively pursuing the experimental construction of this oscillator. While we expect that a more detailed mechanistic model will have to be built to fit data and to guide experiments (in particular once the decay/recovery reaction mechanisms are identified), our analysis of this simple model provides useful insights in the potential of this circuit for oscillations.

REFERENCES

[1] J. Kim, K. S. White, and E. Winfree, "Construction of an *in vitro* bistable circuit from synthetic transcriptional switches," *Molecular systems biology*, vol. 2, no. 1, 2006.

[2] E. Franco, E. Friedrichs, J. Kim, R. Jungmann, R. Murray, E. Winfree, and F. C. Simmel, "Timing molecular motion and production with a synthetic transcriptional clock," *Proceedings of the National Academy of Sciences*, vol. 108, no. 40, pp. E784–E793, 2011.

[3] G. Seelig, D. Soloveichik, D. Y. Zhang, and E. Winfree, "Enzyme-free nucleic acid logic circuits," *Science*, vol. 314, no. 5805, pp. 1585–1588, 2006.

[4] K. Montagne, R. Plasson, Y. Sakai, T. Fujii, and Y. Rondelez, "Programming an in vitro DNA oscillator using a molecular networking strategy," *Molecular Systems Biology*, vol. 7, no. 1, pp. –, 2011.

[5] D. Soloveichik, G. Seelig, and E. Winfree, "DNA as a universal substrate for chemical kinetics," *Proceedings of the National Academy of Sciences*, vol. 107, no. 12, pp. 5393–5398, 2010.

[6] V. Mardanlou, C. H. Tran, and E. Franco, "Design of a molecular bistable system with RNA-mediated regulation," in *Proceedings IEEE Conference on Decision and Control*, 2014.

[7] A. D. Ellington and J. W. Szostak, "In vitro selection of RNA molecules that bind specific ligands," *Nature*, vol. 346, pp. 818–822, 1990.

[8] S. Ohuchi, Y. Mori, and Y. Nakamura, "Evolution of an inhibitory RNA aptamer against T7 RNA polymerase," *FEBS open bio*, 2012.

[9] Y. Mori, Y. Nakamura, and S. Ohuchi, "Inhibitory RNA aptamer against SP6 RNA polymerase," *Biochemical and Biophysical Research Communications*, vol. 420, no. 2, pp. 440–443, 2012.

[10] J. Kim and E. Winfree, "Synthetic *in vitro* transcriptional oscillators," *Molecular Systems Biology*, vol. 7, p. 465, 2011.

[11] D. Angeli and E. Sontag, "Monotone control systems," *IEEE Transactions on Automatic Control*, vol. 48, no. 10, pp. 1684–1698, 2003.

[12] F. Blanchini and E. Franco, "Structurally robust biological networks," *BMC Systems Biology*, vol. 5, no. 1, p. 74, 2011.

[13] C. Cosentino and D. Bates, *Feedback Control in Systems Biology*. CRC Press, 2012.

[14] L. Edelstein-Keshet, *Mathematical Models in Biology*, ser. Classics in applied Mathematics, vol. 46. Philadelphia: SIAM, 2005.

[15] B. Novak and J. J. Tyson, "Design principles of biochemical oscillators," *Nature Reviews Molecular Cell Biology*, vol. 9, no. 12, pp. 981–991, 2008.

[16] J. L. Vinkenborg, N. Karnowski, and M. Famulok, "Aptamers for allosteric regulation," *Nature Chemical Biology*, vol. 7, no. 8, pp. 519–527, 2011.

[17] E. J. Cho, J.-W. Lee, and A. D. Ellington, "Applications of Aptamers as Sensors," *Annual Review of Analytical Chemistry*, vol. 2, pp. 241–264, 2009.

[18] D. Y. Zhang and G. Seelig, "Dynamic DNA nanotechnology using strand-displacement reactions," *Nature Chemistry*, vol. 3, no. 2, pp. 103–113, 2011.

[19] R. Srzednicki, "On rest points of dynamical systems," *Fundamenta Mathematicae*, vol. 126, no. 1, pp. 69–81, 1985.

[20] D. Richeson and J. Wiseman, "A fixed point theorem for bounded dynamical systems," *Illinois J. Math.*, vol. 46, no. 2, pp. 491–495, 2002.

[21] ——, "Addendum to: "A fixed point theorem for bounded dynamical systems" [*Illinois J. Math.*, vol. 46, no. 2, pp. 491–495, 2002]," *Illinois J. Math.*, vol. 48, no. 3, pp. 1079–1080, 2004.

[22] E. Franco, G. Giordano, P.-O. Forsberg, and R. M. Murray, "Negative autoregulation matches production and demand in synthetic transcriptional networks," *ACS Synthetic Biology*, vol. 3, no. 8, pp. 589–599, 2014.

[23] F. Blanchini, E. Franco, and G. Giordano, "A structural classification of candidate oscillatory and multistationary biochemical systems," *Bulletin of Mathematical Biology*, to appear.

[24] R. Clewley, W. Sherwood, M. LaMar, and J. Guckenheimer, "PyDSTool, a software environment for dynamical systems modeling," *URL http://pydstool. sourceforge. net*, 2007.